Journal of Membrane Science & Research

journal homepage: www.msrjournal.com

Research Paper

Creating Bipolar Junction by Depositing Ultrathin Anion-Exchange Coating on Cation-Exchange Membrane to Dissociate Water in Electrodialysis

Muhammad Ahmad [1,*], Shabbir Hussain [2,**], Muhammad Amin Abid [3], Asad Mumtaz [4], Muhammad Ibrar [5], Saz Muhammad [6]

[1] *Department of Chemistry, Division of Science and Technology, University of Education, Lahore 44770, Pakistan*
[2] *Department of Chemistry, Khwaja Fareed University of Engineering and Information Technology, Rahim Yar Khan, Pakistan*
[3] *Department of Chemistry, University of Sahiwal, Sahiwal, Pakistan*
[4] *Department of Chemistry, School of Natural Sciences, National University of Sciences and Technology, Islamabad, Pakistan*
[5] *Department of Chemistry, Lahore Garrison University, DHA Phase VI, Lahore, Pakistan*
[6] *Department of Chemistry, Kohsar University, Murree 47150, Punjab, Pakistan*

Article info

Received 2021-10-05
Revised 2021-11-02
Accepted 2021-11-22
Available online 2021-11-22

Keywords

Nafion
Anion-exchange coatings
Layer-by-layer deposition
Bipolar junction
Water splitting

Highlights

- Anion-exchange films were fabricated from PAH/PSS polyelectrolytes.
- Cation-exchange membranes with anion-exchange films behave as bipolar membranes.
- PAH/PSS films switch their character from anion- to cation-exchange at basic pH.
- Nafion coated with anion-exchange films produces no transport of ions.

Graphical abstract

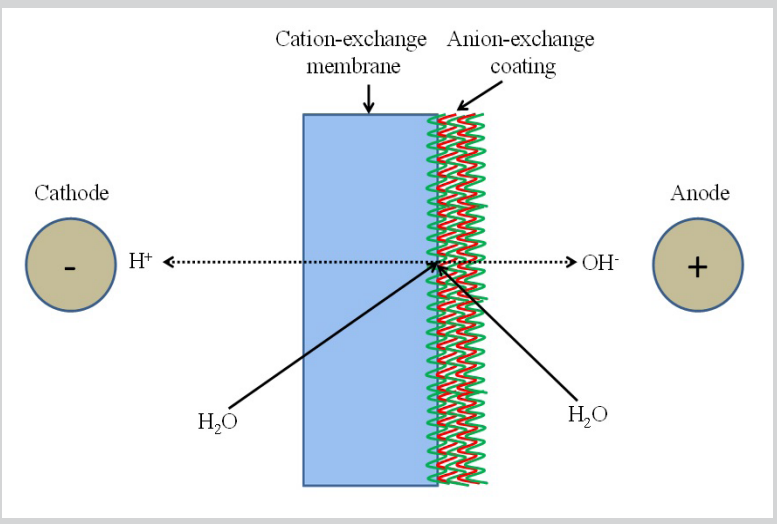

Abstract

Ultrathin anion-exchange films have been created by employing layer-by-layer (LBL) deposition method. The LBL deposited protonated poly(allylamine) (PAH)/poly(4-styrenesulfonate) (PSS) polyelectrolyte multilayers (PEMs) behave as anion-exchange films when PAH and PSS polyelectrolyte solutions are prepared in NaSCN as a supporting electrolyte (SE). Reflectance FTIR studies indicate that when PAH is prepared in 0.5 M NaSCN and PSS is prepared in 1 M NaSCN, the thickness of the film and the number of anion-exchange sites in the film are manifold greater than those in the film fabricated from PAH and PSS polyelectrolytes when either of them is prepared in 0.5 M NaSCN. Transmembrane potential measurements were performed to measure the permselectivity of thus fabricated PEMs. These measurements indicate that the fabricated films demonstrate high anion-exchange properties at neutral pH. However, the ion-exchange character of the films switches from anions- to cations-exchange when pH of the surrounding solutions changes from 7 to 8.4. Diffusion dialysis results through the coated alumina membranes confirm such a change in the net charge of the films with a change in the pH. Current density-voltage curve studies indicate plenty of formation of H^+ and OH^- ions through water dissociation occurring at the interfacial bipolar junction created by depositing these anion-exchange coatings on Nafion cation-exchange membrane (CEM). Donnan dialysis studies also indicate the formation of bipolar junction through deposition of such films on cation-exchange membranes.

1. Introduction

Ion-exchange membranes (IEMs) are of prime importance in the electrodialysis (ED) process. The fundamental studies on electro-membrane processes based on IEMs began almost sixty years ago [1,2]. Since then, IEMs are being employed in ED separations such as salts recovery from waste solution [3], treatment of waste water effluents [4], selective separations of monovalent and divalent ions [5-8], demineralization of milk by products [9], desalination of brackish water [2,10], and pre-concentration of brines [11]. A continuous advancement in the field of IEMs has broadened

* Corresponding author: dr.muhammad.ahmad@ue.edu.pk (M. Ahmad); shabchem786@gmail.com (S. Hussain)

DOI: 10.22079/JMSR.2021.540358.1502

their characteristics and range of applications. Among different types of IEMs, bipolar membranes (BPMs) have attracted much attention of the scientists [12]. A BPM actually consists of two layers laminated together: a cation-exchange layer (CEL) and an anion-exchange layer (AEL) [13]. CEL is negatively charged and thus is only permeable for cations, whereas AEL is positively charged and therefore permits only anions to pass through it. The interfacial region between CEL and AEL is called "bipolar junction" [14]. Contrary to CEMs and anion-exchange membranes (AEMs), BPMs are not supposed to produce any transport of ions across them [15]. The major purpose of BPMs is to produce H^+ and OH^- ions [16]. Under an applied potential, water dissociates into hydroxide ions and protons at the bipolar junction through a disproportionation reaction. It is important to note that no gas is formed during electro-dissociation of water and thus water dissociation and water splitting (at electrodes during electrodialysis) are two different processes [17]. In BPMs literature, the terms "water splitting" and "water dissociation" are frequently employed interchangeably [18].

To ensure the flux of protons and hydroxide ions along the electric field, a BPM is oriented such a way that the CEL faces the cathode and the AEL faces the anode (please see Figure 1) [19-21]. As a BPM is not permeable either for cations or anions [22], the ionic current through a BPM is not supported by ions in the bulk solution under an applied potential [15]. Therefore, the electro-dissociation of H_2O at the bipolar junction yields H^+ and OH^- ions which carry current across the BPM. The generated H^+ ions leave the CEL and move towards the cathode. On the other hand, OH^- ions travel towards the anode after leaving the AEL [21,23]. Such a movement of ions generates base on one side of the BPM and acid on its other side [24, 25]. Currently, AEM and CEM materials are being used in water splitting electrolyzers [26]. The combination of AEMs and CEMs provides separation between anolyte and catholyte while maintaining ionic conduction. Water splitting through bipolar membranes can be used to convert salts into their corresponding acid/base, acidification, water purification, organic synthesis, and alkalisation [27-29]. Use of BPM in ED is an environmental friendly technique and has economical competence advantages as well [30]. In some applications, BPM were used to sustain a pH gradient and H^+ and OH^- ions generated through BPM were ingested at the respective electrodes in ED. This type of ED is helpful for hydrogen production [31,32]. For water dissociation, several microfluidic researches were conducted to make an optimal design of the BPMs [33-36].

The rate of dissociation of water in ED across the BPM due to the presence of polymeric phases of opposite charges is fifty million times faster than the H_2O dissociation in aqueous solutions [37, 38]. The characteristics of interfacial layer play a significant role in the water dissociation at bipolar junction [31,37,39]. The performance of a BPM can be tuned by introducing a water dissociation catalyst, by changing the density of ionic groups at the interfacial region [40], by altering the composition of AEM [41], and by adjusting the structural roughness of bipolar membrane junction [37]. For interfacial region, different inorganic materials [42-44], poly(4-vinylpyridine) and poly(acrylic acid) polyelectrolyte complex [45], polyvinyl alcohol [46], metallic salt $CrCl_3$ [43], polyethylene glycol [47], and graphene oxide were investigated as catalysts for water dissociation at the interfacial region. The interfacial region of the BPM should offer a maximum electrical conductance, provide an efficient linkage with layers to avert the separation of the cation-exchange and anion-exchange parts of the BPM and finally should act as a catalyst in the presence of corresponding base and the weak acids.

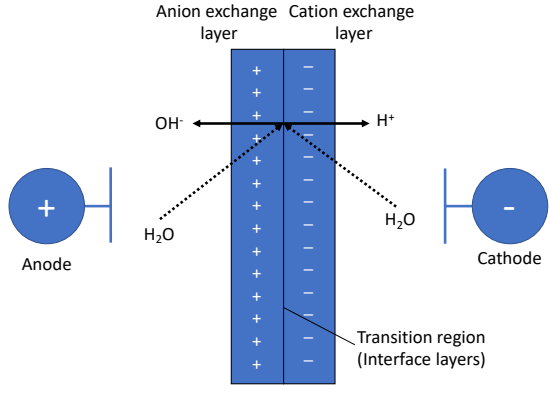

Fig. 1. A schematic structural and functional representation of a bipolar membrane.

In this study, we have created a bipolar junction by depositing AEC on a CEM rather than using the traditional method of laminating CEL and AEL together. Thus, the created interfacial region provides excellent connection between the AEC and the CEM, while minimizing the electrical resistance of the BPM. We prepared PAH and PSS polyelectrolyte solutions using NaSCN as a SE. To create anion-exchange coatings on cation-exchange membranes, we employed LBL deposition of PAH/PSS polyelectrolytes onto Nafion CEMs.

2. Materials and methods

2.1. Materials

Poly(sodium 4-styrenesulfonate) (Mw=70,000 Da), Poly(allylamine hydrochloride) (Mw=17,500 Da), NaCl, and NaSCN were received from Sigma-Aldrich. $NaNO_3$ and KCl were obtained from J. T . Baker. KNO_3, $Mg(NO_3)_2$, and $NaClO_4$ were procured from Jade Scientific. $NaHCO_3$ was acquired from Columbus Chemical. All salts were employed in experiments as acquired. To make all solutions, DI H_2O (Milli-Q reference Ultra-pure Water Purification System, 18 MΩ cm) was employed. The pH values of the solutions of polyelectrolytes were regulated by employing 0.1 M hydrochloric acid and 0.1 M sodium hydroxide solutions. Nafion 115 CEMs were purchased from Ion Power (New Castle, DE, thickness 127 µm). 3-Mercaptopropionic acid (MPA, 99%) (Aldrich) was used as obtained. Porous alumina membranes of 25 mm diameter and 0.02 micrometer surface pore size were procured from Whatman.

2.2. Immobilization of anion-exchange coatings and their characterization

Silicon wafers coated with Au (24 mm × 11 mm) were immersed in an ethanolic solution of 3 mM MPA for 12 hours. Wafers were rinsed with deionized (DI) water and ethanol, and dried with N_2 gas to deposit a monolayer of MPA on the Au surface. PEMs consisting of $(PAH/PSS)_5PAH$ (five bilayers of PAH and PSS capped with a layer of PAH) films were deposited on the MPA modified Si wafers coated with Au. To deposit each layer of polyanion (from 0.02 M PSS, pH ~2.3) and polycation (from 0.02 M PAH, pH ~2.3), wafers were soaked in each solutions of polyelectrolyte for 7 minutes. The repeat unit concentrations are the concentrations of polyelectrolytes. After depositing each layer, wafers were rinsed with DI H_2O to remove loosely bound polyelectrolytes. The type and concentrations of SEs (used in polyelectrolyte solutions) were varied to optimize and maximize the anion-exchange sites in the coatings. Reflectance FTIR spectroscopy (Thermo Nicolet 6700 FTIR spectrometer) was used to characterize the immobilized coatings assembled on above wafers. The data were represented in pseudoabsorbance (noted as absorbance (A) = -log R, where R is the relative reflectance).

Porous alumina membranes were pretreated by keeping them in UV/O_3 (Jelight Model) for 12 minutes. The modification of alumina membranes was carried out in an O-ring holder by exposing just the feed side of alumina to the PAH, PSS and rinsing solutions. Unlike gold wafers, 6 bilayers of PAH and PSS polyelectrolytes were deposited on alumina membranes. Alumina is slightly positively charged [48] and therefore PSS becomes the first layer to be deposited.

A mechanical die was used to punch Nafion membranes into 25 mm disks. For pretreatment, Nafion membranes were oxidized by employing a procedure reported in the literature [49-52], where they were boiled in in 3% H_2O_2, DI H_2O, 1.0 M H_2SO_4 and finally in DI H_2O for thirty minutes sequentially. After oxidation and before modification, membranes were rinsed and stored in DI H_2O. For modification five and half bilayers of PAH and PSS polyelectrolytes were deposited using similar method of LBL deposition. Just like alumina membranes, only one side of Nafion membranes was modified in the same O-ring holder by exposing only one side of the membranes to the rinsing and polyelectrolyte solutions. Images of PEMs coated Nafion membranes before and after current density-voltage measurement experiments were taken with a Magellan (Field Emission Scanning Electron Microscope). For drying, the membrane samples were kept under vacuum at room temperature and were then sputter coated prior to imaging with a 2 nm thick layer of iridium.

2.3. Transmembrane potential measurements

To examine the permselectivity of fabricated anion-exchange coatings, measurements of transmembrane potentials across coated alumina membranes were performed. For these measurements, a two compartment cell was employed, where a coated alumina membrane separated the receiving and source phases. To measure the developed electrical potential across a membrane, a multimeter was used whose terminals were attached to silver/silver-chloride reference electrodes (3.0 M KCl, CH Instruments). The

electrodes were sealed in Haber-Luggin capillaries. The capillaries came nearer to within 4 mm of the alumina membrane. The measurements of transmembrane potential at neutral pH were carried out by employing KCl solutions. The concentrations of KCl solutions were changed from 0.02 to 0.1 M in the source phase, whereas 0.01 M KCl was always used as the receiving phase. The same experiment was repeated while employing $NaHCO_3$ solutions in the receiving and source phases to determine the permselectivity of fabricated films at a basic pH. Both phases (source and receiving) were shaken very strongly during the experiment to decrease the effect of static diffusion boundary layers. Before measuring transmembrane potentials, both capillaries were kept in the receiving phase to measure a minor potential drop between Ag/AgCl electrodes. Later, these small values were subtracted from the readings of multimeter. Next, from the multimeter readings the junction potential values in the capillaries were also subtracted to determine the exact potential difference across the membrane [53]. The activities of various salt solutions were calculated by multiplying the activity coefficients and concentration [54,55].

2.4. Current density-voltage (I-V) curves

I-V curves were acquired by employing the same electrochemical cell used in the measurements of transmembrane potentials. Two Pt wires were inserted into the source and receiving compartments and a potentiostat (CH instrument, model 604) generated a constant current across the electrodes. Throughout measurements, the concentration variance near the membrane's surface was decreased by keeping both the receiving and source phases stirred very strongly. The Ag/AgCl reference electrodes were sealed in Haber-Luggin capillaries, which then extended to within four millimeter of the membrane's surface, so that the voltage drop between the membrane and the two electrodes through the solution during potential measurements across the membrane remains minimum. For a 0-6 mA cm^{-2} range of current densities, the electrical potential difference between Ag/AgCl electrodes was measured to determine the voltage drop across the bare or PEMs coated Nafion membranes. In these experiments, the source and receiving compartments contained 0.05 M NaCl to determine *I-V* curves. The curves were recorded for 3 different membrane sets. The replicas show resistance variation as the standard deviations of values.

2.5. Diffusion and Donnan dialysis

Two homemade glass cells of 100-mL volume were used in diffusion dialysis experiments (Figure 2). An O-ring was used to sandwich and clamp the alumina membranes between the cells. The experimental setup exposes an area of 1.8 cm^2 to the solutions. A strong stirring was used again to decrease the concentration variance near the membrane's surface in both the compartments. The experiments were performed for 2 hours. The ions' transport from source to the receiving phase was measured by withdrawing one milliliter aliquots periodically from the receiving phase. Ion chromatography (Thermo Dionex ICS-5000 Ion Chromatograph) was used to measure the concentrations of anions (Cl^- and SO_4^{2-}), where a 7 anion standard solution (ThermoFisher) was employed to generate calibration curves.

For Donna dialysis, the same two compartment cell was used, where either an unmodified or a modified Nafion CEM was sandwiched in between the compartments. The concentrations of potassium and magnesium ions were determined through inductively coupled plasma-optical emission spectroscopy, (ICP-OES, 152 PrkinElmer Optima 8000 Prep 3) using calibration curves. The transport of ions through membranes was observed as a function of time by plotting total moles of ions permeating to the receiving phase against the dialysis time. Fluxes of ions were determined by dividing the slopes of these linear curves with the membrane's area. Finally, the selectivity of an ion over the other ion was calculated by dividing the flux of one ion with that of the other ion. Standard deviations from three replicate membranes were represented as uncertainties in fluxes and selectivities.

3. Results and discussion

The purpose of this study is to develop a bipolar junction that will catalyze the process of water dissociation into protons and hydroxide ions under an applied potential. We hope to create an ultrathin anion-exchange coating on a CEM with the help of LBL deposition of PAH and PSS polyelectrolytes prepared in NaSCN SE, so that the coated CEM could behave as a bipolar membrane. This section first presents reflectance FTIR results which indicate the creation of anion-exchange coatings when PAH and PSS polyelectrolyte solutions are prepared in NaSCN as a SE. Transmembrane potential measurements and current-voltage curves also confirm the behavior of thus fabricated films as anion-exchange coatings. Diffusion dialysis through alumina and Donnan dialysis through Nafion membranes further provide an insight into the ion-exchange characteristics of the fabricated anion-exchange coatings.

3.1. Reflectance FTIR studies of LBL deposited coatings

We used reflectance FTIR spectroscopy to examine the effect of varied NaSCN supporting electrolyte concentrations on the creation and optimization of anion-exchange sites in the LBL deposited PEMs. We employed NaSCN as a SE with the hope that SCN^- is a strong ligand and will complex with the positively charged ammonium groups of PAH polyelectrolyte [56]. The PSS solution was also prepared in NaSCN SE. Though NaSCN does not form any complexes with the PSS polyelectrolyte, but it helps to avoid the lynching effect due to which SCN^- ions present in the deposited PAH layers might get replaced with the anions of other supporting electrolyte (e.g. with the Cl^- ions coming from NaCl). Thus, lynching effect can increase the electrostatic forces of attractions between the neighboring oppositely charged layers of PEMs and the number of bindings between SCN^- and ammonium groups of PAH polyelectrolyte will decrease. Such a decrease in the number of bindings between SCN^- and ammonium groups will lead to a decreased thickness of the film and hence the number of anion-exchange sites in PEMs [57-59].

First we prepared each of the PAH and PSS polyelectrolyte solution in 0.5 M NaSCN, deposited $(PAH/PSS)_5PAH$ (5 bilayers of PAH and PSS polyelectrolytes capped with a layer of PAH) PEMs, and took the reflectance FTIR spectrum. The spectrum has been shown in Figure 3. Next, we increased the concentration of NaSCN to 1 M. The purpose of increasing the concentration of NaSCN as a SE was to bind more ammonium groups of PAH polyelectrolyte with the SCN^- ions and thus to maximize the number of anion-exchange sites in the polyelectrolyte multilayers as well as the thickness of film. Unfortunately, PAH polyelectrolyte solution in 1 M NaSCN gave a cloudy appearance which most probably was due to formation of a large number of complexes between ammonium groups of PAH and SCN^- ions. Therefore, we used 0.5 M NaSCN concentration for the preparation of PAH polyelectrolytes whereas we increased the concentration of NaSCN to 1 M to make PSS polyelectrolytes solution. We were expecting that the use of 1 M rather than 0.5 M NaSCN will still help in maximizing the number of anion-exchange sites and the thickness of anion-exchange coating. Because the SCN^- ions, due to their higher concentration in PSS solution, will complex with some of the ammonium groups of already assembled PAH layers by thus changes some of the electrostatic forces of attractions (between PAH and PSS) into SCN^--ammonium group bindings.

As shown in the Figure 3, a peak due to SCN^- ions appeared at about 2050 cm^{-1} in the reflectance FTIR spectrum [60,61]. The intensity of the peak was almost 5-6 times greater for the PEMs synthesized from PAH (in 0.5 M NaSCN) and PSS (in 1 M NaSCN) polyelectrolytes than the intensity of the peak for PEMs made from PAH (in 0.5 M NaSCN) and PSS (in 0.5 M NaSCN) polyelectrolytes. This indicates that the concentration of SCN^- in former PEMs is much greater than the concentration of SCN^- in the later PEMs. Therefore, we can conclude that the number of anion-exchange sites in the former PEMs is much greater than the anion-exchange sites present in the later PEMs.

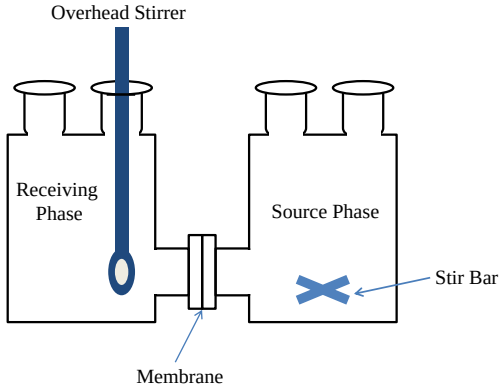

Fig. 2. Diffusion and Donnan dialysis cell is made up of two 100 mL glass compartments joined together by 2.5 centimeter #15 flat joints with the help of an o-ring.

Using reflectance FTIR studies, we examined the anion-exchange aptitude of the $(PAH/PSS)_5PAH$ PEMs prepared with PAH (in 0.5 M NaSCN) and PSS (in 1 M NaSCN). We soaked the PEMs coated wafer in 0.5 M $NaClO_4$ solution for 30 minutes and took the reflectance FTIR spectrum after rinsing it with DI H_2O and drying it with N_2 gas. As shown in Figure 4, the peak due to SCN^- at 2050 cm^{-1} disappeared and a new peak due to ClO_4^- ions appeared at almost 1100 cm^{-1} [62,63]. Next, we soaked the wafer in 0.5 M NaSCN solution for 30 minutes, dried the wafer again with N_2 gas after rinsing it with DI H_2O and took the reflectance FTIR spectrum. As Figure 4 demonstrates, the peak due to ClO_4^- ions disappeared, whereas the older peak due to SCN^- appeared again at 2050 cm^{-1}. These experiments indicate the presence of anion-exchange sites in the PEMs coated on MPA modified Au coated Si wafers. These experiments were repeated three times and similar results were obtained.

We also performed a control experiment by depositing $(PAH/PSS)_5PAH$ PEMs on an MPA modified Au-coated Si wafer, where PAH and PSS both were made in 0.5 M NaCl solutions. The obtained reflectance FTIR spectrum is shown in Figure 5. We repeated the same protocol, where we soaked the wafer in 0.5 M $NaClO_4$ solution for 30 minutes and observed the reflectance FTIR spectrum after rinsing it with DI H_2O and drying it with N_2. There was no change observed in the spectrum. We again soaked the wafer in 0.5 M NaSCN solution for 30 minutes, rinsed it with DI H_2O and dried it with N_2 gas. Again, we could not observe any change in the spectrum. These experiments indicate that the PEMs fabricated from PAH and PSS polyelectrolyte solutions, while using NaCl as a supporting electrolyte, do not contain any anion-exchange sites. Therefore, we can conclude that anion-exchange sites are formed when NaSCN is used as a supporting electrolyte for the preparation of PAH and PSS polyelectrolytes solutions.

3.2. Transmembrane potential measurements

The evidence of the sign of a membrane's net fixed charges can be provided by measuring the permselectivity of that membrane, which can be determined by taking different salt concentrations across two sides of a membrane. We deposited $(PSS/PAH)_6$ PEMs on alumina membranes, where PAH was prepared in 0.5 M NaSCN and PSS was prepared in 1 M NaSCN. The measurements of transmembrane potentials were performed across PEMs-coated alumina membranes to study the ion-exchange features of PEMs. Though slightly positively charged, alumina does not show much permselectivity [48]. Equation 1 expresses the electrical potential difference "E" that arises across a membrane due to difference of salt activities (a_1 and a_2) [64]. Equation 2 expresses the transference number "t_t" which is portion of the current carried by an ion "*i*" across the membrane [54]. In Equation 1, "t_+" is the transference number of cations, "t_-" is the transference numbers of anions, "z_+" is the charge on cations, and "z_-" is the charge on anions. In Equation 2, "z_t", "u_i", and "C_i" are the charge, mobility and concentration of ion "*i*" respectively.

$$E = \left[\frac{t_+}{z_+} + \frac{t_-}{z_-}\right] \frac{2.303\ RT}{F}\ log\ \frac{a_1}{a_2} \quad (1)$$

$$t_i = \frac{z_i u_i C_i}{\sum_{i=1}^{n} z_i u C_i} \quad (2)$$

For an ideal AEM, $t_+ = 0$ and $t_- = 1$ [65]. Figure 6 demonstrates the transmembrane potential measurements through $(PSS/PAH)_6$-coated alumina membranes for two solutions of different pH values. We chose KCl solution to measure transmembrane potentials at pH 7 (neutral pH), whereas we selected $NaHCO_3$ solution to determine transmembrane potentials at pH 8.4 (a basic pH). (The differences in aqueous mobilities of cations and anions in each salt are <12% [54].) Blue diamonds in the Figure 6 are for the transmembrane potential measurements taken through alumina membrane coated with $(PSS/PAH)_6$ PEMs, where 0.5 M NaCl was used as a SE in the preparation of PSS and PAH polyelectrolytes. Such PEMs at neutral pH typically have a positive charge and thus are anions selective [53]. Importantly, the anion transference numbers (t_-) are much higher for the PEMs, when polyelectrolyte solutions were prepared with NaSCN as a SE (0.5 M NaSCN for PAH, and 1 M NaSCN for PSS). In Figure 6, numbers provided above the triangle symbols and below the square symbols are the t_- values. These anions selective PEMs become cations selective at pH 8.3, when the solutions in the source and receiving phases change from KCl to $NaHCO_3$. These experiments indicate that the PAH/PSS PEMs behave as anions selective at neutral pH. The anion-exchange character of PEMs prepared from PAH and PSS polyelectrolyte solutions made in NaSCN is much greater than the anion-exchange character of the PEMs prepared from PAH and PSS polyelectrolyte solutions made in NaCl as a SE. However, with a small increase in the pH of surrounding solutions from 7 to 8.4, the character of the PEMs changes from anions to cations selective. Such a change in the ion-exchange character of the PEMs with a change in pH is attributed to the conversion of charged ammonium groups (at pH 7) into neutral ammine groups (at pH 8.4) [7].

3.3. Current density-voltage (I-V) curves

The $(PAH/PSS)_5PAH$-coatings from the PAH/PSS polyelectrolyte solutions made in NaSCN SE likely behave as anion-exchange layers. To create a bipolar junction, we deposited such coatings on a Nafion CEM, which under an applied electric potential may dissociate water molecules into H^+ and OH^- ions. To observe water splitting phenomenon, we measured the *I-V* curves. There are three distinct regions in a typical *I-V* curve: "Ohmic", "plateau", and "overlimiting" regions [66]. At low current densities, the "Ohmic region" is obtained. In Ohmic region, the drop in potential values escalates linearly with an increase in the current density across a membrane. Second distinct region is called "plateau region", where the potential drop across the membrane escalates rapidly with an increase in the current density values. Third and final region is called "overlimiting region". In this region, multiple phenomenons such as electro-convection and water splitting increase the current again.

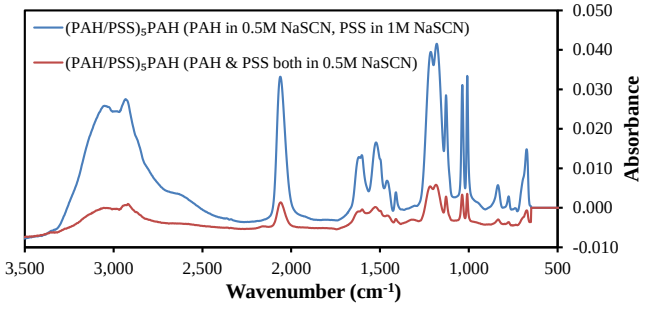

Fig. 3. Reflectance FTIR spectra of the $(PAH/PSS)_5PAH$ PEMs deposited on MPA modified Au-coated silicon wafers. The polyelectrolytes were prepared in different concentrations of NASCN SE as has been mentioned in the legend of the figure.

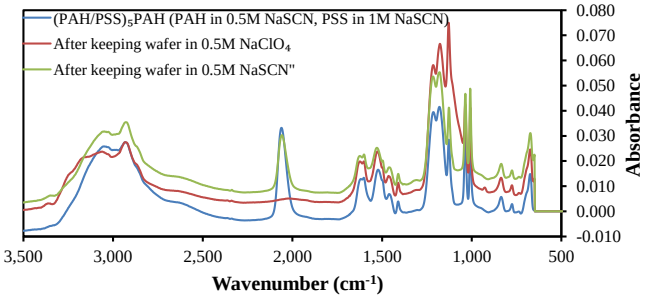

Fig. 4. The change in reflectance FTIR spectra of PEMs when Au-coated wafers were soaked in 0.5 M $NaClO_4$ solutions and then again in 0.5 M NaSCN solutions. The PEMs were fabricated from PAH and PSS solutions made in 0.5 M and 1 M NaSCN respectively.

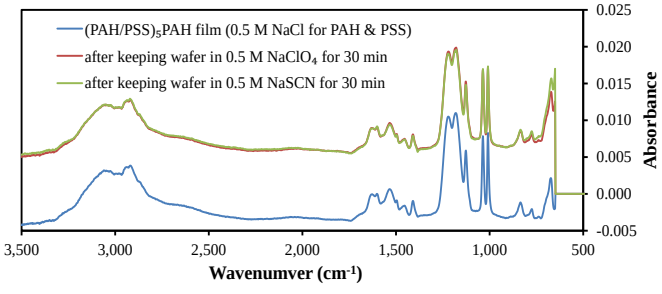

Fig. 5. A control experiment showing the effect of $NaClO_4$ and NaSCN on the reflectance FTIR spectrum of PEMs assembled from LBL deposition of PAH and PSS polyelectrolyte solutions prepared in 0.5 M NaCl as a SE.

Figure 7 presents *I-V* curves for unmodified and $(PAH/PSS)_5PAH$-coated Nafion CEMs at neutral pH. (The PAH and PSS solutions were prepared in 0.5 M and 1 M NaSCN respectively.) A 0.05 M NaCl solution was employed on both sides of the membrane. As can be seen from the Figure 7, coated membrane shows higher resistance as compared to the resistance through a bare Nafion membrane. Upto 0.6 mA cm^{-2} current density values, the potential drop across the coated Nafion increases linearly (Ohmic region). At current density values > 0.6 mA cm^{-2}, the coated membrane demonstrates higher voltage drop across the membrane and thus a "plateau region" is obtained. The overlimiting region starts at ~1.9 mA cm^{-2}, where the process of water dissociation starts occurring. The voltage drop across the membrane at current density values greater than 1.9 mA cm^{-2} but lesser than 3 mA cm^{-2} the voltage drop across the coated Nafion stops increasing or even starts decreasing (please see Figure 7). Such a decrease in the voltage drop across the membrane indicates an abundant supply of additional charges which carry current across the membrane and thus a decrease in the resistance through the membrane is observed. These additional charges (H^+ and OH^- ions) come from the dissociation of water and carry current across the membrane while migrating to the respective electrodes. When the applied current density values are greater than 3 mA cm^{-2}, the phenomenon of water dissociation stops occurring and the voltage drop across the membrane escalates linearly with an increase in the current density. We repeated the experiment 3 times and observed the same *I-V* curves. We also performed a second experiment on the same coated membrane, where we discarded the old solutions and filled new source and receiving phases. In the second experiment on the same coated membrane, the water splitting process could not be observed. These experiments suggest that once the value of current density increases above 3 mA cm^{-2}, probably some permanent changes happen in the coating.

We took SEM images to make sure that the film was not degrading under high current density values. The SEM images are shown in Figure 8. Figure 8 (A) shows that the polyelectrolyte multilayers possibly cover the entire exposed surface of membranes. Actually, one of the important characteristics of LBL deposition method is conformal coating of complex 3-D shapes. The small nodules can be seen in the Figure 8A and B which are likely the polyelectrolyte complexes that fabricate during LBL coating process. The presence of nodules in both Figure 8A and B suggests that the film was not degrading during *I-V* measurements and therefore can still be seen on the membrane. Thus, these experiments suggest that the coated membrane behaves as a bipolar membrane and has potential to produce a lot of H^+ and OH^- ions through water dissociation under an applied potential. However at higher current density values (greater than 3 mA cm^{-2}), likely a permanent change happens in the coating and water splitting stops occurring. We also explored the effect of varied NaCl concentrations on the *I-V* curves. When we increased the concentration of NaCl in the receiving and source phases, the process of water splitting occurred at higher current density values and when we decreased the concentration of NaCl, the water dissociation occurred at lower current density values. We employed 0.5 M NaCl as an optimum concentration to have enough conductivity of source and receiving phases during the ED process as well as to observe the phenomenon of water dissociation at relatively lower current density values.

3.4. Measurement of Cl^-/SO_4^{2-} selectivity through coated alumina in diffusion dialysis

We performed diffusion dialysis experiments through alumina membranes modified with $(PSS/PAH)_6$ PEMs to measure their Cl^-/SO_4^{2-} selectivity. (PAH and PSS solutions were prepared in 0.5 and 1 M NaSCN respectively.) In these experiments, we employed a two compartment cell, where one compartment served as a source phase and the other compartment served as a receiving phase. We employed a source phase containing 0.02 M concentration with respect to each NaCl and Na_2SO_4. The fluxes of Cl^- and SO_4^{2-} and Cl^-/SO_4^{2-} selectivities are provided in Table 1. The Cl^-/SO_4^{2-} selectivity measured through a bare alumina membrane was 2.2. However, after coating the alumina membranes with anion-exchange films, the Cl^- and SO_4^{2-} fluxes decreased. The decrease in SO_4^{2-} flux was proportionately greater than the decrease in the flux of SO_4^{2-} ions. Therefore, Cl^-/SO_4^{2-} selectivity increased from 2.2 to 4.1. As suggested by transmembrane potential measurements, we performed diffusion dialysis through coated alumina at pH 8.4 to confirm a change in the characteristics of the film from anions to cations selective with a change in pH from 7 to 8.4. We employed the same source phase that contained 0.02 M concentration with respect to each NaCl and Na_2SO_4, whereas we used 0.02 M $NaHCO_3$ in the receiving phase. The results of these experiments are shown in Table 2. In these experiments, the Cl^-/SO_4^{2-} selectivity increased further to ~11. Such an increase in the selectivity indicates a change in the native charge of the coating from positive to negative. Due to an increased negative surface charge, divalent SO_4^{2-} experience higher electrostatic forces of repulsion than the monovalent Cl^- and thus the Cl^-/SO_4^{2-} selectivity increases. A comparison of these results with already reported data suggests that our fabricated AECs are comparatively less monovalent to divalent anions selective as compared to the PEMs fabricated from the PAH/PSS polyelectrolytes prepared in NaCl solutions [6]. In addition, AECs when coated on AEMs will demonstrate higher values of limiting currents because of lower concentration polarization near the membrane's surface.

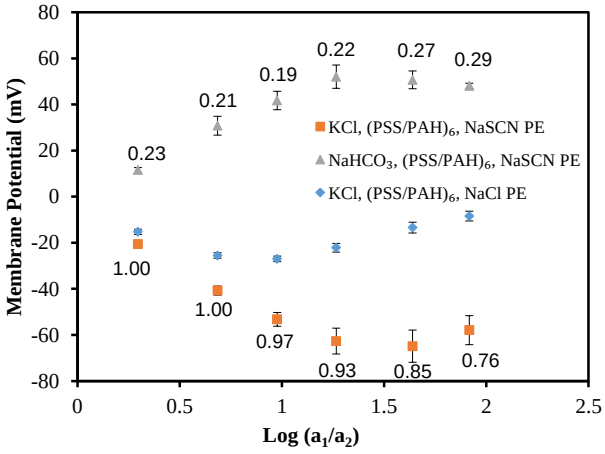

Fig. 6. Measurement of transmembrane potentials across $(PSS/PAH)_6$-coated alumina membranes. Measurements taken through $(PSS/PAH)_6$-coated alumina membranes, with $NaHCO_3$ (pH 8.4) and KCl (pH 7) solutions employed on both sides of the membrane are shown in triangles and squares respectively. These coatings were prepared from PSS and PAH solutions made in 1 M and 0.5 M NaSCN respectively. Diamonds represent the transmembrane potentials through $(PSS/PAH)_6$-coated alumina membranes fabricated from PAH and PSS polyelectrolytes prepared in 0.5 M NaCl. Numbers above the triangle symbols and below the square symbols are the t. values. Deviations from mean values with three different membranes are shown with error bars.

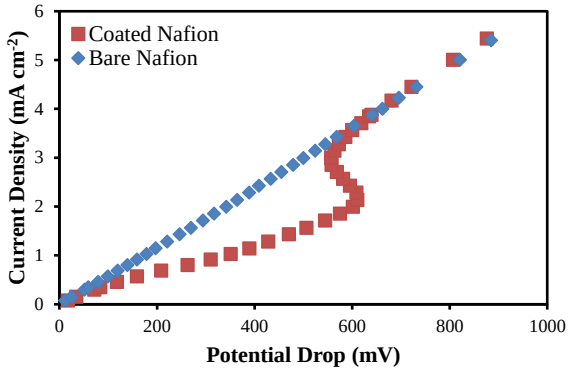

Fig. 7. Potential drop versus current densities plots for Bare and $(PAH/PSS)_5PAH$ coated Nafion CEMs, where PAH solution was prepared in 0.5 M NaSCN and PSS solution was prepared in 1 M NaSCN. For these measurements, a two compartment cell was used and 0.05 M NaCl solution was employed as source as well as receiving phase.

3.5. Measurement of K^+/Mg^{2+} selectivity through coated Nafion in Donnan dialysis

We performed Donnan dialysis through unmodified and $(PAH/PSS)_5PAH$-coated Nafion CEMs. For Donnan dialysis, we used the same two compartment cell, where one compartment contained source phase (0.01 M with respect to each KNO_3 and $Mg(NO_3)_2$) and the other compartment contained receiving phase (0.01 M with respect to $NaNO_3$). The K^+/Mg^{2+} fluxes and selectivities are provided in Table 3. When PEMs are composed of PAH and PSS polyelectrolytes prepared in 0.5 M NaCl solution

each, the film yields a K^+ flux of 0.50 nmol cm^{-2} s^{-1} value, whereas Mg^{2+} flux goes undetected. In Donnan dialysis, the K^+ ions move from source to the receiving phase due to concentration gradient across the Nafion CEM and in turn Na^+ ions move from receiving to the source phase to maintain electrical neutrality in both the source and receiving compartments. If the deposited PEMs behave as anion-exchange coating, then the coated Nafion CEMs should block the transport of cations either from source to the receiving or from receiving to the source phase. When coatings are prepared from PAH/PSS polyelectrolyte solutions prepared in NaSCN as a SE, The fluxes of both K^+ and mg^{2+} go undetected. Therefore, these Donnan dialysis experiments indicate that the $(PAH/PSS)_5PAH$ coatings, where PAH and PSS polyelectrolyte solutions were prepared in NaSCN SE, behaves as an anion-exchange layers. Thus we can conclude that when such coatings are deposited on Nafion cation-exchange membranes, the coated Nafion behaves as a bipolar membrane and does not produce any transport of ions across it.

In a nut shell, an effective way of fabricating BPMs by using LBL deposition of polyelectrolytes on CEMs has been proposed in this study. The *I-V* curves clearly demonstrate the effectiveness of the fabricated bipolar junctions, where the process of water splitting starts occurring at current density values even lower than 2 mA cm^{-2}. At current density values ranging between 1.6 and 2 mA cm^{-2}, a continuous decrease in the resistance clearly indicates plenty of formation of H^+ and OH^- ions through dissociation of H_2O which makes this study first of its kind and unique. Earlier studies on fabrication of BPMs report the method of lamination of CEL and AEL together to generate bipolar junctions [15,17,19,37,67,68].

4. Conclusions

Reflectance FTIR studies indicate that the $(PAH/PSS)_5PAH$ PEMs from PAH and PSS polyelectrolytes prepared in NaSCN SE solutions behave as anion-exchange coatings. The concentration of NaSCN is much important and determines the thickness of film as well as the number of anion-exchange sites in the film. Transmembrane potential measurements also support the FTIR results and show that the aforementioned coatings efficiently behave as anion-exchange layers at neutral pH. However, as shown in the transmembrane potential measurements, such coatings behave as cation-exchange layers when pH of the surrounding solutions changes from neutral to 8.4. Nafion cation-exchange membrane behaves as a bipolar membrane when is coated with such an anion-exchange film. The *I-V* curves show that Nafion coated with these anion-exchange coatings produce a lot of water splitting under an applied electrical potential. Diffusion dialysis studies through alumina membrane indicate that the anion-exchange coatings are almost 4 times more selective for monovalent over divalent anions and that the films net charge changes from positive to negative with a change in pH of the surrounding solutions from 7 to 8.4. Donnan dialysis studies support our claim that a bipolar junction is created when such anion-exchange layers are deposited on CEMs because no net transport of ions was observed through coated Nafion membranes.

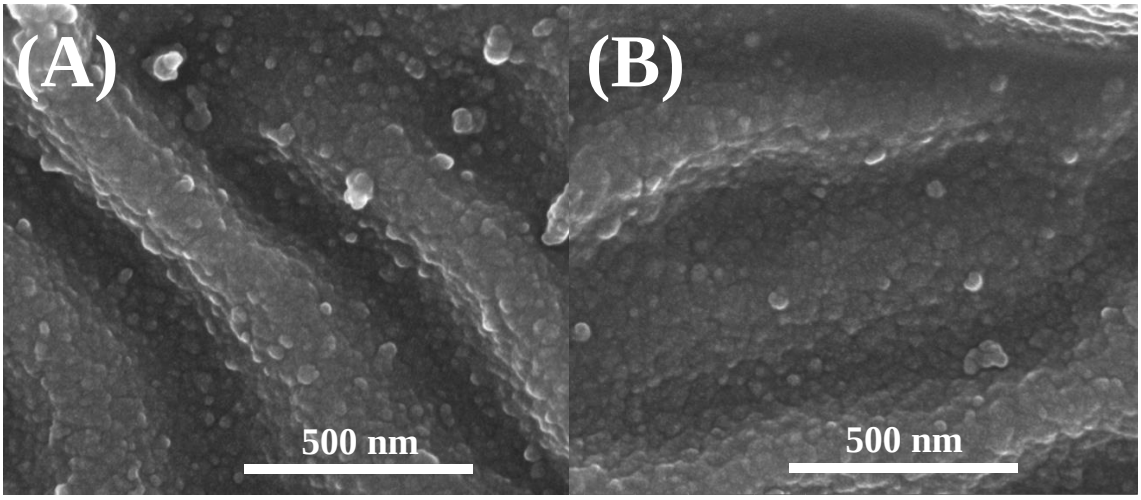

Fig. 8. SEM images of a coated Nafion membrane (A) before and (B) after conducting the current density-voltage (*I-V*) curve experiment.

Table 1
Cl^-/SO_4^{2-} fluxes and selctivities through unmodified and $(PSS/PAH)_6$-coated alumina. The equilibration of membranes was achieved by soaking them in feed solution for 24 hours. The feed solution was 0.02 M with respect to each NaCl and Na_2SO_4. DI H_2O was employed as a receiving phase in these experiments. PEMs were fabricated from PAH & PSS solutions made in NaSCN as a SE.

	Cl^- flux (nmol cm^{-2} s^{-1})	SO_4^{2-} flux (nmol cm^{-2} s^{-1})	Cl^-/SO_4^{2-} selectivity
Bare alumina	9.15 ± 0.20	4.12 ± 0.14	2.2 ± 0.1
Coated alumina	5.84 ± 0.36	1.42 ± 0.24	4.1 ± 0.2

Table 2
Cl^-/SO_4^{2-} fluxes and selctivities through unmodified and $(PSS/PAH)_6$-coated alumina. The equilibration of membranes was achieved by soaking them in feed solution for 24 hours. The feed solution was 0.02 M with respect to each NaCl and Na_2SO_4. 0.02 M $NaHCO_3$ (pH 8.4) was employed as a receiving phase in these experiments. PEMs were fabricated from PAH & PSS solutions made in NaSCN as a SE.

	Cl^- flux (nmol cm^{-2} s^{-1})	SO_4^{2-} flux (nmol cm^{-2} s^{-1})	Cl^-/SO_4^{2-} selectivity
Bare alumina	8.25 ± 0.19	3.90 ± 0.12	2.1 ± 0.1
Coated alumina	5.91 ± 0.67	0.61 ± 0.24	10.7 ± 5.3

Table 3
K^+/Mg^{2+} fluxes and selctivities through unmodified and $(PAH/PSS)_5PAH$-coated Nafion CEMs. For equilibration, membranes were immersed in feed solution for 24 hours prior to their use in Donnan dialysis. The feed solution was 0.0l M with respect to each KNO_3 and $Mg(NO_3)_2$. 0.01 M $NaNO_3$ was employed as a receiving phase. PEMs were fabricated from PAH & PSS solutions made in NaSCN as a SE.

	K^+ flux (nmol cm^{-2} s^{-1})	Mg^{2+} flux (nmol cm^{-2} s^{-1})	K^+/Mg^{2+} selectivity
Bare Nafion	7.75 ± 0.20	2.00 ± 0.11	3.9 ± 0.1
Coated Nafion (NaCl SE)	0.50 ± 0.02	Not detected	>1000
Coated Nafion (NaSCN SE)	Not detected	Not detected	-

References

[1] R. Nagarale, G. Gohil, V.K. Shahi, Recent developments on ion-exchange membranes and electro-membrane processes. Adv. Colloid Interface Sci. 119 (2006) 97-130. DOI: 10.1016/j.cis.2005.09.005.

[2] S. Al-Amshawee, M.Y.B.M. Yunus, A.A.M. Azoddein, D.G. Hassell, I.H. Dakhil, H.A. Hasan, Electrodialysis desalination for water and wastewater: A review.

Chem. Eng. J. 380 (2020) 122231. DOI: 10.1016/j.cej.2019.122231.

[3] D. Babilas, P. Dydo, Zinc salt recovery from electroplating industry wastes by electrodialysis enhanced with complex formation. Sep. Sci. Technol. 55 (2020) 2250-8. DOI: 10.1080/01496395.2019.1664582.

[4] L. Gurreri, A. Tamburini, A. Cipollina, G. Micale, Electrodialysis applications in wastewater treatment for environmental protection and resources recovery: A systematic review on progress and perspectives. Membranes 10 (2020) 146. DOI: 10.3390/membranes10070146.

[5] Y. Zhu, M. Ahmad, L. Yang, M. Misovich, A. Yaroshchuk, M.L. Bruening, Adsorption of polyelectrolyte multilayers imparts high monovalent/divalent cation selectivity to aliphatic polyamide cation-exchange membranes. J. Membr. Sci. 537 (2017) 177-85. DOI: 10.1016/j.memsci.2017.05.043.

[6] M. Ahmad, C. Tang, L. Yang, A. Yaroshchuk, M.L. Bruening, Layer-by-layer modification of aliphatic polyamide anion-exchange membranes to increase Cl^-/SO_4^{2-} selectivity. J. Membr. Sci. 578 (2019) 209-19. DOI: 10.1016/j.memsci.2019.02.018.

[7] M. Ahmad, A. Yaroshchuk, M.L. Bruening, Moderate pH changes alter the fluxes, selectivities and limiting currents in ion transport through polyelectrolyte multilayers deposited on membranes. J. Membr. Sci. 616 (2020) 118570. DOI: 10.1016/j.memsci.2020.118570.

[8] L. Yang, C. Tang, M. Ahmad, A. Yaroshchuk, M.L. Bruening, High selectivities among monovalent cations in dialysis through cation-exchange membranes coated with polyelectrolyte multilayers. ACS Appl. Mater. Interfaces 10 (2018) 44134-44143. DOI: 10.1021/acsami.8b16434.

[9] A. Merkel, A.M. Ashrafi, J. Ečer, Bipolar membrane electrodialysis assisted pH correction of milk whey. J. Membr. Sci. 555 (2018) 185-96. DOI: 10.1016/j.memsci.2018.03.035.

[10] J.M. Ortiz, J.A. Sotoca, E. Expósito, F. Gallud, V. Garcia-Garcia, V. Montiel, A. Aldaz, Brackish water desalination by electrodialysis: batch recirculation operation modeling. J. Membr. Sci. 252 (2005) 65-75. DOI: 10.1016/j.memsci.2004.11.021.

[11] Q.-B. Chen, H. Ren, Z. Tian, L. Sun, J. Wang, Conversion and pre-concentration of SWRO reject brine into high solubility liquid salts (HSLS) by using electrodialysis metathesis. Sep. Purif. Technol. 213 (2019) 587-98. DOI: 10.1016/j.seppur.2018.12.018.

[12] C. Huang, T. Xu, Electrodialysis with bipolar membranes for sustainable development. Environ. Sci. Technol. 40 (2006) 5233-43. DOI: 10.1021/es060039p.

[13] R. Pärnamäe, S. Mareev, V. Nikonenko, S. Melnikov, N. Sheldeshov, V. Zabolotskii, H. Hamelers, M. Tedesco, Bipolar membranes: A review on principles, latest developments, and applications. J. Membr. Sci. 617 (2021) 118538. DOI: 10.1016/j.memsci.2020.118538.

[14] S.Z. Oener, M.J. Foster, S.W. Boettcher, Accelerating water dissociation in bipolar membranes and for electrocatalysis. Science 369 (2020) 1099-103. DOI: 10.1126/science.aaz1487.

[15] J.C. Bui, I. Digdaya, C. Xiang, A.T. Bell, A.Z. Weber, Understanding Multi-Ion Transport Mechanisms in Bipolar Membranes. ACS Appl. Mater. Interfaces 12 (2020) 52509-26. DOI: 10.1021/acsami.0c12686.

[16] S. Mareev, E. Evdochenko, M. Wessling, O. Kozaderova, S. Niftaliev, N. Pismenskaya, V. Nikonenko, A comprehensive mathematical model of water splitting in bipolar membranes: Impact of the spatial distribution of fixed charges and catalyst at bipolar junction. J. Membr. Sci. 603 (2020) 118010. DOI: 10.1016/j.memsci.2020.118010.

[17] S. Chabi, A.G. Wright, S. Holdcroft, M.S. Freund, Transparent bipolar membrane for water splitting applications. ACS Appl. Mater. Interfaces 9 (2017) 26749-55. DOI: 10.1021/acsami.7b04402.

[18] O. Rybalkina, K. Tsygurina, E. Melnikova, G. Pourcelly, V. Nikonenko, N. Pismenskaya, Catalytic effect of ammonia-containing species on water splitting during electrodialysis with ion-exchange membranes. Electrochim. Acta 299 (2019) 946-62. DOI: 10.1016/j.electacta.2019.01.068.

[19] M.L. Jordan, L. Valentino, N. Nazyrynbekova, V.M. Palakkal, S. Kole, D. Bhattacharya, Y.J. Lin, C.G. Arges, Promoting water-splitting in Janus bipolar ion-exchange resin wafers for electrodeionization. Mol. Syst. Des. Eng. 5 (2020) 922-35. DOI: 10.1039/C9ME00179D.

[20] M. Manohar, A.K. Das, V.K. Shahi, Efficient bipolar membrane with functionalized graphene oxide interfacial layer for water splitting and converting salt into acid/base by electrodialysis. Ind. Eng. Chem. Res. 57 (2018) 1129-36. DOI: 10.1021/acs.iecr.7b03885.

[21] G.A. Lindquist, Q. Xu, S.Z. Oener, S.W. Boettcher, Membrane electrolyzers for impure-water splitting. Joule 4 (2020) 2549-2561. DOI: 10.1016/j.joule.2020.09.020.

[22] J. Dai, Y. Dong, P. Gao, J. Ren, C. Yu, H. Hu, Y. Zhu, X. Teng, A sandwiched bipolar membrane for all vanadium redox flow battery with high coulombic efficiency. Polymer 140 (2018) 233-9. DOI: 10.1016/j.polymer.2018.02.051.

[23] B.S. Kim, S.C. Park, D.H. Kim, G.H. Moon, J.G. Oh, J. Jang, M.S. Kang, K.B. Yoon, Y.S. Kang, Bipolar Membranes to Promote Formation of Tight Ice-Like Water for Efficient and Sustainable Water Splitting. Small 16 (2020) 2002641. DOI: 10.1002/smll.202002641.

[24] M.B. McDonald, S. Ardo, N.S. Lewis, M.S. Freund, Use of bipolar membranes for maintaining steady-state ph gradients in membrane-supported, solar-driven water splitting. ChemSusChem 7 (2014) 3021-7. DOI: 10.1002/cssc.201402288.

[25] K. Mani, Electrodialysis water splitting technology. J. Membr. Sci. 58 (1991) 117-38. DOI: 10.1016/S0376-7388(00)82450-3.

[26] B. Yuzer, H. Selçuk, G. Chehade, M.E. Demir, I. Dincer, Evaluation of hydrogen production via electrolysis with ion exchange membranes. Energy 190 (2020) 116420. DOI: 10.1016/j.energy.2019.116420.

[27] M. Kumar, V.K. Shahi, Heterogeneous–homogeneous composite bipolar membrane for the conversion of salt of homologous carboxylates into their corresponding acids and bases. J. Membr. Sci. 349 (2010) 130-7. DOI:10.1016/j.memsci.2009.11.041.

[28] C. Jiang, Y. Wang, T. Xu, An excellent method to produce morpholine by bipolar membrane electrodialysis. Sep. Purif. Technol. 115 (2013) 100-6. DOI: 10.1016/j.seppur.2013.04.053.

[29] Y. Wei, Y. Wang, X. Zhang, T. Xu, Comparative study on the treatment of simulated brominated butyl rubber wastewater by using bipolar membrane electrodialysis (BMED) and conventional electrodialysis (ED). Sep. Purif. Technol. 110 (2013) 164-9. DOI: 10.1016/j.seppur.2013.03.028.

[30] Y. Wei, C. Li, Y. Wang, X. Zhang, Q. Li, T. Xu, Regenerating sodium hydroxide from the spent caustic by bipolar membrane electrodialysis (BMED). Sep. Purif. Technol. 86 (2012) 49-54. DOI: 10.1016/j.seppur.2011.10.019.

[31] M.B. McDonald, M.S. Freund, Graphene oxide as a water dissociation catalyst in the bipolar membrane interfacial layer. ACS Appl. Mater. Interfaces 6 (2014) 13790-7. DOI: 10.1021/am503242v.

[32] N.M. Vargas-Barbosa, G.M. Geise, M.A. Hickner, T.E. Mallouk, Assessing the utility of bipolar membranes for use in photoelectrochemical water-splitting cells. ChemSusChem 7 (2014) 3017-20. DOI: 10.1002/cssc.201402535.

[33] L.-J. Cheng, H.-C. Chang, Switchable pH actuators and 3D integrated salt bridges as new strategies for reconfigurable microfluidic free-flow electrophoretic separation. Lab on a Chip 14 (2014) 979-87. DOI: 10.1039/C3LC51023A.

[34] Z. Slouka, S. Senapati, H.-C. Chang, Microfluidic systems with ion-selective membranes. Annu. Rev. Anal. Chem. 7 (2014) 317-35. DOI: 10.1146/annurev-anchem-071213-020155.

[35] J. De Jong, R.G. Lammertink, M. Wessling, Membranes and microfluidics: a review. Lab on a Chip 6 (2006) 1125-39. DOI: 10.1039/b603275c.

[36] V. Nikonenko, M. Urtenov, S. Mareev, G. Pourcelly, Mathematical modeling of the effect of water splitting on ion transfer in the depleted diffusion layer near an ion-exchange membrane. Membranes 10 (2020) 22. DOI: 10.3390/membranes10020022.

[37] J. Balster, S. Srinkantharajah, R. Sumbharaju, I. Pünt, R.G. Lammertink, D. Stamatialis, M. Wessling, Tailoring the interface layer of the bipolar membrane. J. Membr. Sci. 365 (2010) 389-98. DOI: 10.1016/j.memsci.2010.09.034.

[38] V. Zabolotskii, N. Shel'Deshov, N. Gnusin, Dissociation of water molecules in systems with ion-exchange membranes. Russ. Chem. Rev. 57 (1988) 801. DOI: 10.1070/RC1988v057n08ABEH003389.

[39] Y. Xue, N. Wang, C. Huang, Y. Cheng, T. Xu, Catalytic water dissociation at the intermediate layer of a bipolar membrane: The role of carboxylated Boltorn® H30. J. Membr. Sci. 344 (2009) 129-35. DOI: 10.1016/j.memsci.2009.07.042.

[40] M.-S. Kang, A. Tanioka, S.-H. Moon, Effects of interface hydrophilicity and metallic compounds on water-splitting efficiency in bipolar membranes. Korean J. Chem. Eng. 19 (2002) 99-106. DOI: 10.1007/BF02706881.

[41] C. Jiang, M.M. Hossain, Y. Li, Y. Wang, T. Xu, Ion Exchange Membranes for Electrodialysis: A Comprehensive Review of Recent Advances. J. Membr. Sep. Technol. 3 (2014) 185-205. DOI: 10.6000/1929-6037.2014.03.04.2.

[42] T. Jeevananda, K.-H. Yeon, S.-H. Moon, Synthesis and characterization of bipolar membrane using pyridine functionalized anion exchange layer. J. Membr. Sci. 283 (2006) 201-8. DOI: 10.1016/j.memsci.2006.06.029.

[43] R. Fu, T. Xu, G. Wang, W. Yang, Z. Pan, PEG–catalytic water splitting in the interface of a bipolar membrane. J. Colloid Interface Sci. 263 (2003) 386-90. DOI: 10.1016/S0021-9797(03)00307-2.

[44] R. Simons, Preparation of a high performance bipolar membrane. J. Membr. Sci. 78 (1993) 13-23. DOI: 10.1016/0376-7388(93)85243-P.

[45] H. Strathmann, H.-J. Rapp, B. Bauer, C. Bell, Theoretical and practical aspects of preparing bipolar membranes. Desalination 90 (1993) 303-23. DOI: 10.1016/0011-9164(93)80183-N.

[46] R.-Q. Fu, Y.-H. Xue, T.-W. Xu, W.-H. Yang, Fundamental studies on the intermediate layer of a bipolar membrane Part IV. Effect of polyvinyl alcohol (PVA) on water dissociation at the interface of a bipolar membrane. J. Colloid Interface Sci. 285 (2005) 281-7. DOI: 10.1016/j.jcis.2004.11.050.

[47] A.M. Rajesh, M. Kumar, V.K. Shahi, Functionalized biopolymer based bipolar membrane with poly ethylene glycol interfacial layer for improved water splitting. J. Membr. Sci. 372 (2011) 249-57. DOI: 10.1016/j.memsci.2011.02.009.

[48] M. Robinson, J. Pask, D. Fuerstenau, Surface charge of alumina and magnesia in aqueous media. J. Am. Ceram. Soc. 47 (1964) 516-20. DOI: 10.1111/j.1151-2916.1964.tb13801.x.

[49] W. Xie, R.M. Darling, M.L. Perry, Processing and pretreatment effects on vanadium transport in nafion membranes. J. Electrochem. Soc. 163 (2015) A5084. DOI: 10.1149/2.0111601jes.

[50] R. Kuwertz, C. Kirstein, T. Turek, U. Kunz, Influence of acid pretreatment on ionic conductivity of Nafion® membranes. J. Membrane Sci. 500 (2016) 225-35. DOI: 10.1016/j.memsci.2015.11.022.

[51] B. Jiang, L. Yu, L. Wu, D. Mu, L. Liu, J. Xi, X. Qiu, Insights into the impact of the nafion membrane pretreatment process on vanadium flow battery performance.

ACS Appl. Mater. Interfaces 8 (2016) 12228-38. DOI: 10.1021/acsami.6b03529.

[52] H. Tang, Methanol crossover reduction by Nafion modification via layer-by-layer self-assembly techniques. Colloids Surf, A Physicochem. Eng. Asp. 407 (2012) 49-57. DOI: 10.1016/j.colsurfa.2012.05.006.

[53] C. Cheng, A. Yaroshchuk, M.L. Bruening, Fundamentals of selective ion transport through multilayer polyelectrolyte membranes. Langmuir 29 (2013) 1885-92. DOI: 10.1021/la304574e.

[54] A.J. Bard, L.R. Faulkner, Fundamentals and applications. Electrochem. Methods 2 (2001) 580-632.

[55] J. Kielland, Individual activity coefficients of ions in aqueous solutions. J. Am. Chem. Soc. 59 (1937) 1675-8. DOI: 10.1021/ja01288a032.

[56] Y. Li, S. Fang, X. Wang, L. Zhai, K. Chen, M. Duan, Coacervation of copolymer of diallyldimethylammonium chloride and sodium styrenesulfonate aqueous solution. J. Macromol. Sci. A 55 (2018) 154-60. DOI: 10.1080/10601325.2017.1400893.

[57] S.T. Dubas, J.B. Schlenoff, Swelling and smoothing of polyelectrolyte multilayers by salt. Langmuir 17 (2001) 7725-7. DOI: 10.1021/la0112099.

[58] X. Gong, C. Gao, Influence of salt on assembly and compression of PDADMAC/PSSMA polyelectrolyte multilayers. Phys. Chem. Chem. Phys. 11 (2009) 11577-86. DOI: 10.1039/B915335G.

[59] M. Gopinadhan, O. Ivanova, H. Ahrens, J.-U. Günther, R. Steitz, C.A. Helm, The influence of secondary interactions during the formation of polyelectrolyte multilayers: Layer thickness, bound water and layer interpenetration. J. Phys. Chem. B 111 (2007) 8426-34. DOI: 10.1021/jp067402z.

[60] C. Guha, J.M. Chakraborty, S. Karanjai, B. Das, The structure and thermodynamics of ion association and solvation of some thiocyanates and nitrates in 2-methoxyethanol studied by conductometry and FTIR spectroscopy. J. Phys. Chem. B 107 (2003) 12814-9. DOI: 10.1021/jp030731w.

[61] G.-Q. Lu, S.-G. Sun, L.-R. Cai, S.-P. Chen, Z.-W. Tian, K.-K. Shiu, In situ FTIR spectroscopic studies of adsorption of CO, SCN-, and poly (o-phenylenediamine) on electrodes of nanometer thin films of Pt, Pd, and Rh: Abnormal infrared effects (AIREs). Langmuir 16 (2000) 778-86. DOI: 10.1021/la990282k.

[62] Y. Chen, Y.-H. Zhang, L.-J. Zhao, ATR-FTIR spectroscopic studies on aqueous LiClO4, NaClO 4, and Mg (ClO 4) 2 solutions. Phys. Chem. Chem. Phys. 6 (2004) 537-42. DOI: 10.1039/B311768E.

[63] Y. Zhang, F. Ding, L. Zhao, FTIR-ATR chamber for observation of efflorescence and deliquescence processes of NaClO 4 aerosol particles on ZnSe substrate. Chin. Sci. Bull. 50 (2005) 2149-52. DOI: 10.1007/BF03182662.

[64] E.A. Guggenheim, The conceptions of electrical potential difference between two phases and the individual activities of ions. J. Phys. Chem. 33 (2002) 842-9. DOI: 10.1007/BF03182662.

[65] J.T. Vardner, T. Ling, S.T. Russell, A.M. Perakis, Y. He, N.W. Brady, S.K. Kumar, A.C. West, Method of measuring salt transference numbers in ion-selective membranes. J. Electrochem. Soc. 164 (2017) A2940. DOI: 10.1149/2.0321713jes.

[66] P. Ramirez, H. Rapp, S. Reichle, H. Strathmann, S. Mafé, Current-voltage curves of bipolar membranes. J. Appl. Phys. 72 (1992) 259-64. DOI: 10.1063/1.352124.

[67] L. Bazinet, F. Lamarche, D. Ippersiel, Bipolar-membrane electrodialysis: Applications of electrodialysis in the food industry. Trends Food Sci. Technol. 9 (1998) 107-13. DOI: 10.1016/S0924-2244(98)00026-0.

[68] F.P. Chlanda, L.T. Lee, K.-J. Liu. Bipolar membranes and method of making same. Google Patents; 1978.